Bol. Soc. Paran. Mat.
©SPM – E-ISSN-2175-1188
SPM: www.spm.uem.br/bspm

(3s.) **v. 2026 (44) 12** : 1–12.
ISSN-0037-8712
doi:10.5269/bspm.80653

Variational Physics-Informed Neural Networks for the $p(x)$-Laplacian Problem

Hamdi Braiek*

ABSTRACT: In this paper, we study a variational physics-informed neural network (VPINN) for solving the $p(x)$-Laplacian equation with Dirichlet boundary conditions. The proposed method builds a neural network that automatically satisfies the boundary values and minimizes the energy of the problem. The loss function is computed using Monte Carlo sampling, and derivatives are obtained with automatic differentiation. To train the network, we use two steps: first the Adam optimizer, then the L-BFGS method for faster convergence. We test the approach on several examples in one and two dimensions, where the exponent $p(x)$ changes smoothly or has jumps. The results show that the VPINN gives accurate and stable solutions, even when the coefficients vary strongly in space.

Keywords: $p(x)$-Laplacian, nonlinear equation, variable exponent function, PINNs, deep learning, physics-informed neural networks.

Contents

1. Introduction

Nonlinear elliptic equations driven by nonstandard growth operators arise in a wide range of physical and engineering models, including electrorheological fluids, image processing, and nonlinear elasticity [1,5,15,16]. A prominent example is the variable-exponent Laplace operator

$$\Delta_{p(x)}u := \operatorname{div}\left(|\nabla u|^{p(x)-2}\nabla u\right),$$

which generalizes the classical p-Laplacian by allowing the growth exponent p to vary spatially. The associated variable-exponent Lebesgue and Sobolev spaces present several analytical subtleties, for instance, reflexivity, density, and embedding theorems depend critically on the range and regularity of $p(x)$, and a comprehensive treatment of these properties can be found in the standard reference monograph on the subject [10,11,12].

From the viewpoint of analysis, boundary-value problems involving the $p(x)$-Laplacian pose well-known challenges: existence and uniqueness of weak solutions typically rely on monotonicity or pseudomonotonicity frameworks and on precise hypotheses on the exponent $p(x)$. A large literature has developed dedicated existence/regularity results and multiplicity theories for such problems, which illustrates both the mathematical richness and the technical complexity of the model [2,14,22].

* The author has legally changed their name from Hamdi Houichet to Hamdi Braiek. ORCID ID: https://orcid.org/0000-0002-3301-1385

2020 *Mathematics Subject Classification:* 35B10, 65N12, 68T07, 35J20, 65K10.
Submitted December 07, 2025. Published April 21, 2026

On the numerical side, classical discretization techniques like finite elements, finite volumes, spectral methods have been adapted to $p(x)$-type operators [6,9]. They often require careful design of quadrature, mesh refinement near singularities, or tailored nonlinear solvers because the operator is highly nonlinear and possibly degenerate or singular depending on $p(x)$. The increasing complexity of modern applications motivates alternative, mesh-free, and flexible approximation paradigms that can more naturally handle complex geometries, variable coefficients, and data-driven modeling.

Physics-Informed Neural Networks (PINNs) recently emerged as a mesh-free approach to approximate solutions of PDEs by embedding the governing equations and boundary conditions directly into a neural-network loss functional [18,19]. Introduced and popularized in the computational-physics community, the PINN paradigm has demonstrated striking flexibility for forward and inverse problems across fluid dynamics, solid mechanics, and reacting flows [7,8,13,20]. In the seminal formulation, the PDE residual and boundary mismatch are enforced at collocation points and the network parameters are trained so that the residuals become small in a least-squares sense [19].

A natural refinement of the PINN idea is the variational PINN (VPINN) framework, which replaces or complements strong-form residuals by weak or energy functionals [4,17,21]. Variational formulations have several advantages for elliptic and variational PDEs: they allow enforcing conservation or integral identities directly, they provide natural control of function-space norms, and they can be discretized using Monte-Carlo quadrature coupled with neural-network trial spaces. Recent developments on VPINNs and hp-VPINNs have established practical algorithms and begun to analyze the influence of quadrature and test-space choices on convergence behavior [3,4]. These works suggest VPINNs are particularly well suited to nonlinear elliptic problems where an energy principle is available.

Despite the rapid progress in PINN and VPINN methodologies, the numerical solution of variable-exponent problems with neural-network based variational approaches has received relatively little attention. The $p(x)$-Laplacian presents specific difficulties for PINNs/VPINNs: the energy density involves the non-polynomial integrand $|\nabla u|^{p(x)}/p(x)$ whose point-wise behavior depends on both the gradient magnitude and the spatially varying exponent, and the nonlinearity may amplify approximation and optimization errors in ways not captured by analysis for constant-exponent elliptic problems. These aspects motivate a focused study of VPINNs for the $p(x)$-Laplace model.

1.1. Contributions of this work

In this article we develop and investigate a variational PINN strategy for the Dirichlet problem

$$\begin{cases} -\text{div}\left(|\nabla u|^{p(x)-2}\nabla u\right) + V(x)u = f, & \text{in } \Omega, \\ u = g & \text{on } \partial\Omega \end{cases} \tag{1.1}$$

where $\Omega \subset \mathbb{R}^d$, with $d \geq 2$, is an open bounded domain with smooth boundary $\partial\Omega$, V belongs to $L^\infty(\Omega)$ and $v_0 := \text{essinf}_\Omega V(x) > 0$ and the source function $f \in W^{-1,p'(x)}(\Omega)$ with $\frac{1}{p(x)} + \frac{1}{p'(x)} = 1$, with $p \in C(\overline{\Omega})$ satisfies the condition

$$1 < p^- := \inf_{x\in\Omega} p(x) \leq p(x) \leq p^+ := \sup_{x\in\Omega} p(x) \leq 2. \tag{1.2}$$

Our main contributions are, first, to formulate the appropriate variational energy and admissible spaces in the variable-exponent Sobolev setting and show the well-posedness of (1.1). Second, we propose a practical VPINN architecture for the $p(x)$-Laplacian that uses a boundary-lifting to enforce Dirichlet data, Monte-Carlo integration for the interior energy terms, and a two-stage optimizer based on Adam and followed by L-BFGS refinement. The algorithmic design follows best practices from the PINN/VPINN literature and adapts them to the variable-exponent context [4,19]. We finally perform a suite of numerical experiments such as a discontinuous one-dimensional exponent benchmark, a smooth two-dimensional oscillatory exponent on a rectangular domain, and a parameterized two-dimensional on a disk domain to evaluate robustness, accuracy, and the effect of hyperparameters.

1.2. Organization of the paper

The paper is organized as follows. In Section 2 we review variable-exponent function spaces and state the variational formulation of the $p(x)$-Laplacian Dirichlet problem and discuss existence and uniqueness

of the variational solution. Section 3 introduces the VPINN architecture: network lifting for boundary conditions, the variational loss, Monte-Carlo quadrature, and implementation details including automatic differentiation and optimization strategies. In Section 4 we present the numerical experiments described above and a parameter study and compare error metrics. Finally, we finish by concluding remarks and discusses future directions.

2. Setting of the Problem and Well-Posedness

We first present essential definitions and results in Lebesgue and Sobolev spaces with variable exponent functions. During this work, we will assume that the variable-exponent function $p(x)$ satisfies condition (1.2). Let first define the variable-exponent Lebesgue space $L^{p(x)}(\Omega)$ by

$$L^{p(x)}(\Omega) = \{u : \Omega \to \mathbb{R} \text{ measurable such that } \rho_{p(x)}(u) < \infty\}$$

where $\rho_{p(x)}(u) = \int_\Omega |u(x)|^{p(x)} \, \mathrm{d}x$ is a convex modular of u. $L^{p(x)}(\Omega)$ equipped with the Luxembourg norm

$$\|u\|_{L^{p(x)}(\Omega)} = \inf \left\{ \tau > 0 \text{ such that } \rho_{p(x)} \left(\frac{u}{\tau} \right) \leq 1 \right\}$$

is a separable and reflexive Banach space [12].

Similarly, we define the variable-exponent Sobolev space $W^{1,p(x)}(\Omega)$ by

$$W^{1,p(x)}(\Omega) = \{u \in L^{p(x)}(\Omega) \,|\, \nabla u \in L^{p(x)}(\Omega)^d\}.$$

The space $W^{1,p(x)}(\Omega)$, which is equipped with the following norm

$$\|u\|_{1,p(x)} = \|u\|_{L^{p(x)}(\Omega)} + \|\nabla u\|_{L^{p(x)}(\Omega)},$$

is also separable and reflexive Banach space [10].

Note that $W_0^{1,p(x)}(\Omega)$ is the closure of $C_0^1(\Omega)$ in $W^{1,p(x)}(\Omega)$ with respect to the norm $\|u\|_{1,p(x)}$. The space $W_0^{1,p(x)}(\Omega)$ is separable, reflexive, and uniformly convex Banach space (see [12, Theorem 2.1]). For $u \in W_0^{1,p(x)}(\Omega)$, we define an equivalent norm

$$\|u\| = \|\nabla u\|_{1,p(x)},$$

since the Poincaré inequality holds [10], i.e., there exists a positive constant $C_P > 0$ such that

$$\|u\|_{p(x)} \leq C_P \|\nabla u\|_{p(x)} \text{ for all } u \in W_0^{1,p(x)}(\Omega). \tag{2.1}$$

Moreover, we have the compact embedding

$$W^{1,p(x)}(\Omega) \hookrightarrow\hookrightarrow L^{q(x)}(\Omega),$$

if $q \in C^+(\Omega)$ with $q(x) < p^*(x)$ for all $x \in \Omega$, where

$$p^*(x) = \begin{cases} \frac{dp(x)}{d-p(x)} & \text{if } p(x) < d, \\ \infty & \text{if } p(x) \geq d. \end{cases}$$

According to [12, Theorem 1.3], we have:

Proposition 2.1 *For any $u \in W^{1,p(x)}(\Omega)$, we define the potential $\rho_{p(x)}(\nabla u) = \int_\Omega |\nabla u|^{p(x)} \, dx$. Then, we have:*

$$\|\nabla u\|^{p^-}_{L^{p(x)}(\Omega)} \leq \rho_{p(x)}(\nabla u) \leq \|\nabla u\|^{p^+}_{L^{p(x)}(\Omega)}, \quad \text{if} \quad \|\nabla u\|_{L^{p(x)}(\Omega)} \geq 1,$$

$$\|\nabla u\|^{p^+}_{L^{p(x)}(\Omega)} \leq \rho_{p(x)}(\nabla u) \leq \|\nabla u\|^{p^-}_{L^{p(x)}(\Omega)}, \quad \text{if} \quad \|\nabla u\|_{L^{p(x)}(\Omega)} \leq 1.$$

In the sequel, we will establish the existence and uniqueness of a solution for the PDE (1.1). Suppose there exists an extension $G \in W^{1,p(x)}(\Omega)$ with $\operatorname{tr} G = g$ on $\partial\Omega$, define the affine admissible set

$$\mathcal{A} := \{u \in W^{1,p(x)}(\Omega) : \ u - G \in W_0^{1,p(x)}(\Omega)\}$$

Let us define the energy functional

$$F(u) = \int_\Omega \frac{1}{p(x)}|\nabla u|^{p(x)}\,dx + \frac{1}{2}\int_\Omega V(x)u^2\,dx - \langle f, u\rangle, \qquad \forall u \in \mathcal{A}, \tag{2.2}$$

where $\langle\cdot,\cdot\rangle$ denotes the duality pairing between $W^{-1,p'(\cdot)}(\Omega)$ and $W^{1,p(x)}(\Omega)$.

Proposition 2.2 *For fixed $f \in W^{-1,p'(\cdot)}(\Omega)$, the functional (2.2) admits a unique solution $u \in \mathcal{A}$. Moreover, the solution u is exactly the solution to the nonlinear PDE (1.1).*

Proof: Take $u \in \mathcal{A}$, by definition $u \in W^{1,p(x)}(\Omega)$ so the first term in F is finite. Assume $p_- > \frac{2d}{d+2}$, hence $W^{1,p(x)}(\Omega) \hookrightarrow L^2(\Omega)$, we also have $u \in L^2(\Omega)$ with $V \in L^\infty$ and hence the second term is also finite. For all $f \in W^{-1,p'(\cdot)}(\Omega)$, the dual pairing $\langle f, u\rangle$ is well defined. Hence $F(u) \in \mathbb{R}$ for all $u \in \mathcal{A}$.

Now, let $w \in W_0^{1,p(x)}(\Omega)$, write $u = G+w$. We will show that $F(G+w) \to +\infty$ when $\|w\|_{W^{1,p(x)}} \to \infty$. By the Poincaré like-inequality and the embedding $W_0^{1,p(x)} \hookrightarrow L^2$, there exists $C_P > 0$ such that

$$\|w\|_{L^2} \le C_P\|\nabla w\|_{L^{p(x)}}, \qquad \forall w \in W_0^{1,p(x)}(\Omega) \tag{2.3}$$

Since $V \ge v_0 > 0$, and Young's inequality gives for all $\delta_1 = \frac{v_0}{2} > 0$, we have

$$\begin{aligned}\int_\Omega Vu^2dx = \int_\Omega V(G+w)^2dx &\ge v_0\|w\|_{L^2}^2 - 2\|V\|_{L^\infty}\|G\|_{L^2}\|w\|_{L^2} - \|V\|_{L^\infty}\|G\|_{L^2}^2\\ &\ge \delta_1\|w\|_{L^2}^2 - C_{V,G},\end{aligned}$$

where $C_{V,G} = \left(\frac{2\|V\|_{L^\infty}^2}{v_0} + \|V\|_{L^\infty}\right)\|G\|_{L^2}^2$. Apply, (2.3), we get

$$\int_\Omega V(G+w)^2dx \ge \frac{\delta_1}{C_P^2}\|w\|_{W_0^{1,p(x)}}^2 - C_{V,G}. \tag{2.4}$$

Now, using the elementary inequality

$$|a+b|^{p(x)} \ge 2^{1-p_+}|a|^{p(x)} - |b|^{p(x)} \quad \text{for all } a, b \in \mathbb{R}^N,$$

then set $C_G = \int_\Omega \frac{1}{p(x)}|\nabla G|^{p(x)}dx$, we have

$$\int_\Omega \frac{1}{p(x)}|\nabla(w+G)|^{p(x)}dx \ge c_1\int_\Omega |\nabla w|^{p(x)}dx - C_G.$$

where $c_1 = \frac{2^{1-p_+}}{p_+}$. Apply Proposition 2.1, we get

$$\int_\Omega \frac{1}{p(x)}|\nabla(w+G)|^{p(x)}dx \ge C\|w\|_{W_0^{1,p(x)}}^{p_-} - C_G \tag{2.5}$$

Applying Young's inequality, we obtain for any $\varepsilon > 0$

$$|\langle f, w+G\rangle| \le \varepsilon\|w\|_{W^{1,p(x)}}^2 + \frac{1}{4\varepsilon}\|f\|_{W^{-1,p'(\cdot)}}^2 + |\langle f, G\rangle|. \tag{2.6}$$

Putting (2.4), (2.5) and (2.6) together yields

$$F(w+G) \ge C\|w\|_{W_0^{1,p(x)}}^{p_-} + \frac{\delta_1}{2C_P^2}\|w\|_{L^2}^2 - \varepsilon\|w\|_{W^{1,p(x)}}^2 - C',$$

where $C' = \frac{1}{2}C_{V,G} + C_G + |\langle f, G\rangle| + \frac{1}{4\varepsilon}\|f\|^2_{W^{-1,p'(\cdot)}}$. Choose $\varepsilon \in \left(0, \frac{\delta_1}{4C_P^2}\right)$, we can deduce that $F(u) \to +\infty$ as $\|w\|_{W_0^{1,p(x)}} \to \infty$. Thus, F is coercive in the admissible set $\mathcal{A}$.

Let $(u_n) \subset \mathcal{A}$ be a minimizing sequence for F, e.g., $F(u_n) \to \inf_{v\in\mathcal{A}} F(v)$. By coercivity of F the sequence (u_n) is bounded in $W^{1,p(x)}(\Omega)$. Using the reflexivity property of $W^{1,p(x)}(\Omega)$, we can extract a subsequence (still denoted (u_n)) and a function $u \in W^{1,p(x)}(\Omega)$ such that

$$u_n \rightharpoonup u \quad \text{weakly in } W^{1,p(x)}(\Omega).$$

Since $\mathcal{A}$ is an affine, closed subset in $W^{1,p(x)}(\Omega)$, we have $u \in \mathcal{A}$.

We now pass to the limit in F. We since have that, the compact embedding $W^{1,p(x)}(\Omega) \hookrightarrow L^2(\Omega)$ gives that the bounded sequence (u_n) has a subsequence converging strongly in $L^2(\Omega)$ to u. Hence, for $V \in L^\infty$, we get

$$\int_\Omega V u_n^2\, dx \to \int_\Omega V u^2\, dx, \qquad \text{as } n \to \infty.$$

Note that the linear functional $u \mapsto \langle f, u\rangle$ is continuous with respect to the weak topology of $W^{1,p(x)}$, so

$$\langle f, u_n\rangle \to \langle f, u\rangle.$$

Since, the map $u \mapsto \int_\Omega \frac{1}{p(x)}|\nabla u|^{p(x)}dx$ is convex and weakly lower semicontinuous in $W^{1,p(x)}(\Omega)$, these give

$$F(u) \le \liminf_{n\to\infty} F(u_n) = \inf_{v\in\mathcal{A}} F(v),$$

Then u is a minimizer of F in $\mathcal{A}$. The uniqueness of the minimizer follows from the strict convexity of $F(u)$ for any $v_0 > 0$.

Let u be the minimizer of F. Consider any test $v \in W_0^{1,p(x)}(\Omega)$ and for small $t \in \mathbb{R}$, we have:

$$\begin{aligned}\langle F'(u), v\rangle &= \lim_{t\to 0} \frac{F(u+tv) - F(u)}{t} \\ &= \int_\Omega |\nabla u|^{p(x)-2}\nabla u \cdot \nabla v\, dx + \int_\Omega V(x)uv\, dx - \langle f, v\rangle = 0.\end{aligned}$$

Therefore, the functional $F(\cdot)$ is Gâteaux differentiable in $W^{1,p(x)}(\Omega)$ and its unique minimizer is a solution of the weak formulation:

$$\begin{cases}\text{Find } u \in \mathcal{A} \text{ such that:} \\ \displaystyle\int_\Omega |\nabla u|^{p(x)-2}\nabla u \cdot \nabla v\, dx + \int_\Omega V(x)uv\, dx = \langle f, v\rangle \quad \forall v \in W_0^{1,p(x)}(\Omega).\end{cases} \tag{2.7}$$

By integrating by part and using Green formula, we easily get that u is the unique solution to the PDE (1.1). □

3. Physics-Informed Neural Networks

PINNs have emerged as a powerful paradigm for solving both forward and inverse problems governed by PDEs, particularly those exhibiting nonlinearity or ill-posedness [19]. PINNs provide a mesh-free framework to approximate solutions of nonlinear partial differential equations by embedding the governing equations and boundary conditions into the neural network loss function. Rather than relying on labeled data, the learning is guided by the PDE residual or a variational functional and boundary constraints [4,19].

Let $\mathcal{N}(\cdot;\Theta)$ be a fully-connected feed-forward neural network with L layers, widths n_ℓ and parameters

$$\Theta = \{W^{(l)}, b^{(l)} :\ l = 1, \dots, L\},$$

where $W^{(\ell)} \in \mathbb{R}^{n_\ell \times n_{\ell-1}}$ and $b^{(\ell)} \in \mathbb{R}^{n_\ell}$ are the weights matrix and the biases, respectively. The core idea of PINNs, as introduced in [19], is to approximate the unknown solution $u(x)$ of the variational energy

(2.2), for a given $x \in \Omega$, via a neural function u_Θ, where $u_\Theta(x) := N^L_\Theta(x)$. is the output of a feed-forward neural network given for a smooth activation function σ defined as follows:

$$\begin{aligned} \text{input layer:} \quad & N^0_\Theta(x) = x \in \mathbb{R}^d, \\ \text{hidden layers } 1 \le l \le L-1: \quad & N^l_\Theta(x) = \sigma(W^l z^{l-1}(x) + b^l) \in \mathbb{R}^{N_l}, \\ \text{output layer:} \quad & N^L_\Theta(x) = W^L z^{L-1}(x) + b^L \in \mathbb{R}. \end{aligned}$$

We denote the trainable neural network with free parameters Θ by $N_\Theta(x) = \mathcal{N}(x;\Theta)$. Let $\mathcal{U}_\Theta = \{u_\Theta : \Theta \in \mathbb{R}^P\}$ denote the family of neural trial functions with $P = \sum_{l=1}^L N_l(N_{l-1}+1)$. Then, to enforce Dirichlet boundary conditions strongly we use a lifting

$$u_\Theta(x) = G(x) + B(x)N_\Theta(x), \tag{3.1}$$

where G is a prescribed extension of the boundary data satisfying $\operatorname{Tr} G = g$ on $\partial\Omega$ and B is a smooth boundary factor that vanishes on $\partial\Omega$. With this lifting the Dirichlet condition is satisfied exactly whenever G matches the trace. We replace u the solution of the energy F in (2.2) by the neural approximation u_Θ, we define the variational PINN interior loss $\mathcal{L}_{\text{int}}$ and the boundary mismatch penalty $\mathcal{L}_{\text{b}}$ by

$$\begin{aligned} \mathcal{L}_{\text{int}}(\Theta) &= \frac{1}{|\Omega|}\int_\Omega \left(\tfrac{1}{p(x)}|\nabla u_\Theta|^{p(x)} + \frac{1}{2}V(x)u_\Theta^2 - u_\Theta\right) dx, \\ \mathcal{L}_{\text{b}}(\Theta) &= \frac{1}{|\partial\Omega|}\int_{\partial\Omega} |u_\Theta - g|^2 \, ds, \end{aligned}$$

The total training loss is then

$$\mathcal{L}(\Theta) = \mathcal{L}_{\text{int}}(\Theta) + \lambda_b \mathcal{L}_{\text{b}}(\Theta), \tag{3.2}$$

where $\lambda_b > 0$ balances the boundary enforcement. In practice we approximate the integrals $\mathcal{L}_{\text{int}}$ and $\mathcal{L}_{\text{b}}$ by Monte-Carlo sums on the collocation sets $X_{\text{int}} = \{x_i\}_{i=1}^{M_{\text{int}}} \subset \Omega$, and $X_{\text{b}} = \{x_j\}_{j=1}^{M_{\text{b}}} \subset \partial\Omega$. The empirical loss is

$$\widetilde{\mathcal{L}}(\Theta) = \frac{1}{M_{\text{int}}}\sum_{i=1}^{M_{\text{int}}} \left[\tfrac{1}{p(x_i)}|\nabla u_\Theta(x_i)|^{p(x_i)} + \frac{1}{2}V(x_i)u_\Theta(x_i)^2 - f(x_i)u_\Theta(x_i)\right] + \frac{\lambda_b}{M_{\text{b}}}\sum_{j=1}^{M_{\text{b}}} |u_\Theta(x_j) - g(x_j)|^2.$$

In order to avoid numerical instability where $|\nabla u_\Theta| \approx 0$, we regularize the gradient norm by $|\nabla u_\Theta|_\varepsilon := \sqrt{|\nabla u_\Theta|^2 + \varepsilon^2}$ with $\varepsilon = 10^{-3}$, and then we use the automatic differentiation to evaluate automatically $\frac{\partial u_\Theta(x)}{\partial x_i}$ by backpropagation.

Note that the discrete training problem is the finite-dimensional minimization

$$\Theta^* = \arg\min_{\Theta \in \mathcal{U}_\Theta} \widetilde{\mathcal{L}}(\Theta). \tag{3.3}$$

In practice we perform optimization in two stages

- Stage 1: We use stochastic gradient methods (Adam) with mini-batching and resampling of collocation points for initial convergence
- Stage 2: We integrate the quasi-Newton refinement (L-BFGS) which starting from the Adam iterate to accelerate convergence to a local minimizer.

Typical hyperparameters to tune are M_{int}, M_{b}, λ_b, network width/depth, and learning rate schedule, see Figure 1 for the diagram of PINNs.

Note that, if the two conditions hold

(A) For every $u \in W^{1,p(x)}(\Omega)$ and every $\delta > 0$ there exists $\Theta \in \mathcal{U}_\Theta$ such that $\|u - u_\Theta\|_{W^{1,p(x)}(\Omega)} < \delta$.

(B) For each fixed network size and for each sample size $M_{\text{int}}, M_{\text{b}}$, let $\Theta_M \in \mathcal{U}_\Theta$ be a minimizer of the empirical loss $\widetilde{\mathcal{L}}(\Theta)$. Suppose the optimizer delivers Θ_M with

$$\widetilde{\mathcal{L}}(\Theta_M) \to \inf_{u \in \mathcal{A}} F(u) \quad \text{as } M_{\text{int}}, M_{\text{b}} \to \infty,$$

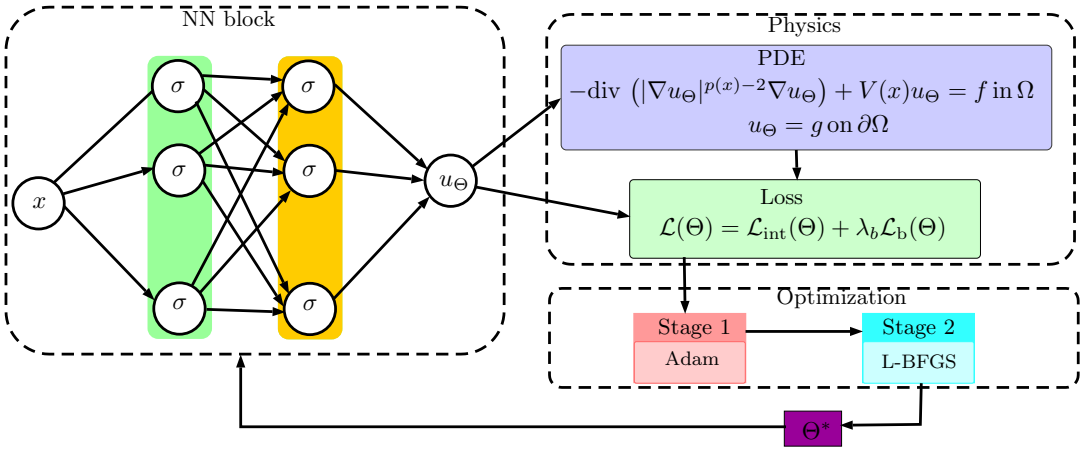

Figure 1: Schematic representation of a PINN for solving (1.1) with nonhomogeneous Dirichlet boundary.

Then, up to extraction of a subsequence, the corresponding network solutions u_{Θ_M} converge weakly in $W^{1,p(x)}(\Omega)$ to the unique variational solution $u^\star$ of (2.2).

Remark 3.1 *We emphasize that (A) is the density of neural networks in Sobolev spaces which is nontrivial and depends on architecture and activation, and (B) requires global or sufficiently good local minimization; therefore the above statement is conditional rather than a rigorous convergence theorem. Still, it provides the conceptual link between the continuous variational problem and the discrete PINN training.*

4. Numerical Tests

In this section, we present three numerical experiments to evaluate the accuracy and robustness of the proposed physics-informed neural network (PINN) framework for solving the nonlinear problem (1.1). We consider one-dimensional and two-dimensional geometries with both regular and nontrivial domains, including a discontinuous exponent, a rectangular domain, and a circular domain. For all tests, the forcing term f is generated by the manufactured solution technique: the analytical expression of u_{true} is substituted into the differential operator, and the corresponding f is computed automatically using automatic differentiation. This ensures that the PINN is trained on data consistent with the governing equation. In order to assess accuracy, we use the relative L^2-error between the learned approximation u_Θ and the analytical solution u_{true}:

$$\mathcal{E}_{L^2} = \frac{\|u_\Theta - u_{\text{true}}\|_{L^2(\Omega)}}{\|u_{\text{true}}\|_{L^2(\Omega)}}.$$

4.1. Test 1: 1D discontinuous exponent

In this first experiment, we consider the one-dimensional domain $\Omega = [-1, 1]$ and define a discontinuous variable exponent

$$p(x) = \begin{cases} 1.5, & \text{if } x < 0, \\ 2.0, & \text{if } x \geq 0, \end{cases}$$

while the potential is fixed to $V(x) = 1$. The manufactured solution is prescribed as $u_{\text{true}}(x) = \sin(\pi x)$, with homogeneous Dirichlet boundary conditions $u(-1) = u(1) = 0$ and the potential is $V(x) = 1$. The source term f is computed automatically from the governing PDE by applying the differential operator to u_{true} using automatic differentiation.

For the training configuration, we set the number of interior collocation points to $M_{\text{int}} = 5000$ and boundary points to $M_{\text{b}} = 1000$. The neural network consists of $L = 4$ layers (three hidden layers) with 40 neurons per hidden layer and tanh activation functions. In the first optimization stage, we employ

the Adam optimizer with an initial learning rate $\eta_1 = 10^{-3}$ and train for 5×10^4 epochs. During the second stage, we switch to the L-BFGS optimizer with the strong Wolfe line search, running up to 3000 iterations. After hyperparameter tuning, the best performance is achieved with 80 neurons per hidden layer, boundary penalty weight $\lambda_b = 10$ (selected from the range $\{1, 10, 50, 100\}$), and learning rate $\eta_1 = 10^{-3}$.

Figure 2 compares the reference solution u_{true} and the PINN approximation u_{Θ^*}. The approximation remains stable across the discontinuity at $x = 0$, which demonstrates the robustness of the network in handling non-smooth coefficients in $p(x)$. The relative L^2 error is found to be $\mathcal{E}_{L^2} = 1.2 \times 10^{-3}$, which confirms the accuracy of the proposed variational PINN approach in the discontinuous-exponent setting.

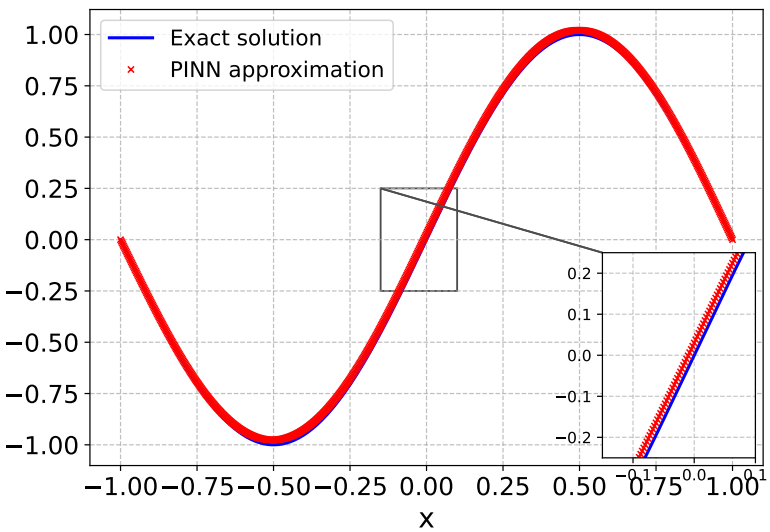

Figure 2: Comparison between the exact and the PINN-approximated solutions for the one-dimensional discontinuous exponent case. The network successfully captures the gradient discontinuity at $x = 0$.

4.2. Test 2: 2D rectangular domain

In this second test, we evaluate the capability of the proposed PINN framework to approximate smooth solutions of the variable-exponent $p(x, y)$-Laplacian in two dimensions. We consider the rectangular domain $\Omega = [0, 2]^2$ and prescribe the analytical manufactured solution

$$u_{\text{true}}(x, y) = \sin(\pi x) \sin(\pi y),$$

with the oscillatory exponent

$$p(x, y) = 1.5 + 0.4 \sin(\pi x) \sin(\pi y),$$

and $V(x, y) = 0$. The forcing term $f(x, y)$ is also obtained from the PDE operator using automatic differentiation. The boundary lifting function is defined as $B(x, y) = (1 - x^2)(1 - y^2)$, which vanishes on $\partial\Omega$.

We employ uniformly distributed random collocation points with $(M_{\text{int}}, M_b) = (10{,}000, 2{,}000)$. The neural network comprises $L = 4$ layers (three hidden layers) with 80 neurons per hidden layer and tanh activation functions. The first optimization stage is performed with the Adam optimizer using a learning rate $\eta_1 = 10^{-3}$ for 8×10^4 epochs, followed by the L-BFGS refinement with the strong Wolfe line search, performing up to 4000 iterations. The boundary penalty coefficient is set to $\lambda_b = 50$.

This configuration is designed to test the accuracy of the PINN model in a smooth two-dimensional setting with a spatially varying exponent. Figure 3 shows the surface plots of the reference and predicted solutions, together with the pointwise absolute error distribution. The predicted solution closely matches the analytical reference, and the isovalues of the pointwise error lie between 0 and 1.75×10^{-2}. The

resulting relative error $\mathcal{E}_{L^2} = 2.3 \times 10^{-3}$, demonstrates the high accuracy and stability of the proposed PINN formulation in capturing oscillatory behavior induced by the variable exponent $p(x, y)$.

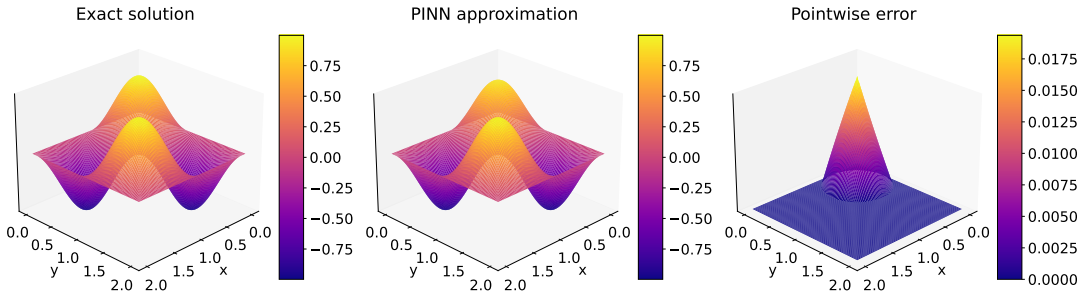

Figure 3: PINN results for the two-dimensional rectangular domain. Left: exact solution; center: predicted solution; right: absolute error $|u_\Theta - u_{\text{true}}|$.

4.3. Test 3: 2D disk

In the third numerical experiment, we consider the circular domain $\Omega = \{(x, y) \in \mathbb{R}^2 : x^2 + y^2 \leq R^2\}$, with $R = 2$. The variable exponent $p(x, y)$ depends on a parameter α and is defined by

$$p^\alpha(x, y) = \begin{cases} 1 + \dfrac{1}{\frac{\alpha}{2}(x + y) + \alpha + 1}, & \alpha \neq 0, \\ 2, & \alpha = 0, \end{cases}$$

while the manufactured analytical solution is given by

$$u^\alpha_{\text{true}}(x, y) = \begin{cases} \dfrac{\sqrt{2}\, e^{\alpha+1}}{\alpha} \left(e^{(\alpha/2)(x+y)} - 1 \right), & \alpha \neq 0, \\ \dfrac{\sqrt{2}e}{2}(x + y), & \alpha = 0. \end{cases}$$

The potential is chosen as $V(x, y) = \alpha$, and the boundary lifting factor is taken as $B(x, y) = R - \sqrt{x^2 + y^2}$, which ensures $B|_{\partial\Omega} = 0$.

The interior collocation points are uniformly sampled inside the disk using the standard polar-to-Cartesian transformation $r = R\sqrt{\hbar}$, and $\theta = 2\pi\vartheta$, where $\hbar, \vartheta \sim \text{Unif}(0, 1)$ are independent uniform random variables. This transformation ensures a uniform distribution of points within the disk. Boundary points are generated uniformly along the circle using random $\theta \in [0, 2\pi]$. We consider $M_{\text{int}} = 10000$ and $M_{\text{b}} = 2000$.

The experiment investigates the effect of the parameter $\alpha \in \{0, 0.5, 1, 1.5, 2\}$ on the accuracy and stability of the learned solution. It also examines the robustness of the variational PINN with respect to strong spatial variations of the exponent $p(x, y)$ between 1 and 2.

The network and training configurations for each case are four layers with 120 neurons each. Figure 4 presents the predicted solutions u^α_Θ and the corresponding relative L^2 errors $\mathcal{E}^\alpha_{L^2} = \frac{\|u^\alpha_\Theta - u^\alpha_{\text{true}}\|_{L^2(\Omega)}}{\|u^\alpha_{\text{true}}\|_{L^2(\Omega)}}$.

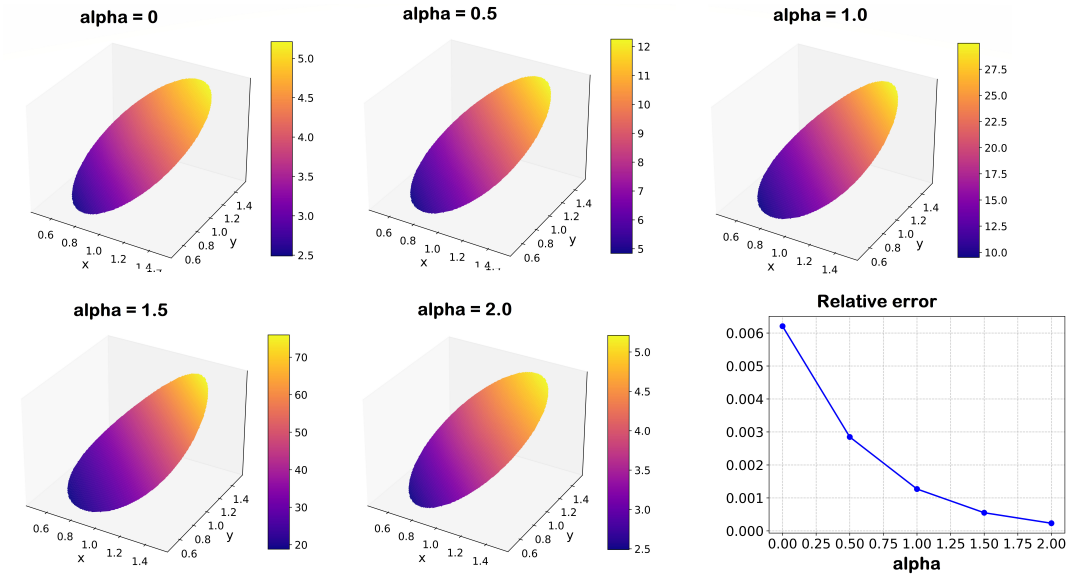

Figure 4: PINN solutions on the disk of radius $R = 2$ for different values of the parameter α. The method remains stable and accurate across varying degrees of nonlinearity in $p^{\alpha}(x, y)$.

The results, summarized in Table 1, confirm that the PINN framework produces stable and accurate approximations for all values of α, which achieve smaller errors as the coefficient field becomes more regular.

Table 1: Relative L^2 error for different values of the parameter α in the disk-domain experiment.

α	0	0.5	1	1.5	2
$\mathcal{E}^{\alpha}_{L^2}$	6.207×10^{-3}	2.848×10^{-3}	1.269×10^{-3}	5.492×10^{-4}	2.307×10^{-4}

Conclusion

In this work, we applied a variational physics-informed neural network to solve nonlinear PDEs with variable coefficients. The main idea was to include the variational form of the problem directly in the neural network loss. The VPINN keeps the main advantages of energy-based numerical methods, such as stability and accuracy, but does not need a computational mesh. This makes it easier to use for complex shapes or irregular domains. The numerical tests showed that the method works well for problems with changing or discontinuous exponents. In the future, we plan to study the mathematical convergence of the method in variable-exponent spaces, to design adaptive sampling rules, and to extend the approach to inverse and optimal control problems involving $p(x)$-type operators.

Conflict of Interest The author states that the publishing of this paper does not involve any conflicts of interest.

Ethics approval and consent to participate Not applicable.

Funding Not applicable.

References

1. Acerbi, E., Mingione, G., and Seregin, G. Regularity results for parabolic systems related to a class of non-newtonian fluids. In *Annales de l'Institut Henri Poincaré C, Analyse non linéaire* (2004), vol. 21, Elsevier, pp. 25–60.

2. Alves, C. O., and Barreiro, J. L. Existence and multiplicity of solutions for a $p(x)$-Laplacian equation with critical growth. *Journal of Mathematical Analysis and Applications 403*, 1 (2013), 143–154.

3. Berrone, S., Canuto, C., and Pintore, M. Solving PDEs by variational physics-informed neural networks: an a posteriori error analysis. *Annali dell' Università di Ferrara 68*, 2 (2022), 575–595.

4. Berrone, S., Canuto, C., and Pintore, M. Variational physics informed neural networks: the role of quadratures and test functions. *Journal of Scientific Computing 92*, 3 (2022), 1–27.

5. Braiek, H. Primal-Dual method for image denoising with variable exponent Sobolev spaces. *Moroccan Journal of Pure and Applied Analysis 11*, 2 (2025), 117–133.

6. Breit, D., Diening, L., and Schwarzacher, S. Finite element approximation of the $p(\cdot)$-Laplacian. *SIAM Journal on Numerical Analysis 53*, 1 (2015), 551–572.

7. Cai, S., Mao, Z., Wang, Z., Yin, M., and Karniadakis, G. E. Physics-informed neural networks (pinns) for fluid mechanics: A review. *Acta Mechanica Sinica 37*, 12 (2021), 1727–1738.

8. Cai, S., Wang, Z., Wang, S., Perdikaris, P., and Karniadakis, G. E. Physics-informed neural networks for heat transfer problems. *Journal of Heat Transfer 143*, 6 (2021), 060801.

9. del Teso, F., and Lindgren, E. A finite difference method for the variational p-Laplacian. *Journal of Scientific Computing 90*, 1 (2022), 67.

10. Diening, L., Harjulehto, P., Hästö, P., and Ruzicka, M. *Lebesgue and Sobolev Spaces with Variable Exponents*. Springer, 2011.

11. Edmunds, D. E., and Rákosník, J. Sobolev embeddings with variable exponent. *Studia Mathematica 143*, 3 (2000), 267–293.

12. Fan, X., and Zhao, D. On the spaces $L^{p(x)}$ and $W^{m,p(x)}$. *Journal of Mathematical Analysis and Applications 263*, 2 (2001), 424–446.

13. He, Y., Wang, Z., Xiang, H., Jiang, X., and Tang, D. An artificial viscosity augmented physics-informed neural network for incompressible flow. *Applied Mathematics and Mechanics 44*, 7 (2023), 1101–1110.

14. Ho, K., and Sim, I. Existence results for degenerate $p(x)$-laplace equations with Leray-Lions type operators. *Science China Mathematics 60*, 1 (2017), 133–146.

15. Houichet, H., Theljani, A., and Moakher, M. A nonlinear fourth-order PDE for image denoising in sobolev spaces with variable exponents and its numerical algorithm. *Computational and Applied Mathematics 40*, 3 (2021), 1–29.

16. Houichet, H., Theljani, A., Moakher, M., and Rjaibi, B. A nonstandard higher-order variational model for speckle noise removal and thin-structure detection. *Journal of Mathematical Study 52*, 4 (Nov. 2019), 394–424.

17. Kharazmi, E., Zhang, Z., and Karniadakis, G. E. hp-VPINNs: Variational physics-informed neural networks with domain decomposition. *Computer Methods in Applied Mechanics and Engineering 374* (2021), 113547.

18. Lu, L., Meng, X., Mao, Z., and Karniadakis, G. E. DeepXDE: A deep learning library for solving differential equations. *SIAM review 63*, 1 (2021), 208–228.

19. Raissi, M., Perdikaris, P., and Karniadakis, G. E. Physics-informed neural networks: A deep learning framework for solving forward and inverse problems involving nonlinear partial differential equations. *Journal of Computational physics 378* (2019), 686–707.

20. Raissi, M., Yazdani, A., and Karniadakis, G. E. Hidden fluid mechanics: Learning velocity and pressure fields from flow visualizations. *Science 367*, 6481 (2020), 1026–1030.

21. Shang, Y., Wang, F., and Sun, J. Randomized neural network with Petrov–Galerkin methods for solving linear and nonlinear partial differential equations. *Communications in Nonlinear Science and Numerical Simulation 127* (2023), 107518.

22. Zhang, Q. Existence of solutions for $p(x)$-Laplacian equations with singular coefficients in $\mathbb{R}^N$. *Journal of Mathematical Analysis and Applications 348*, 1 (2008), 38–50.

Hamdi Braiek,

ESPRIT School of Engineering,
18 rue de l'Usine Charguia II 2035 Ariana, Tunisia..

and

University of Tunis El Manar,
National Engineering School of Tunis,
Laboratory for Mathematical and Numerical

Modeling in Engineering Science,
B.P. 37, 1002 Tunis-Belvédère, Tunisia,
ORCID ID: https://orcid.org/0000-0002-3301-1385
E-mail address: hamdi.houichet@gmail.com